DNS OF BOUNDARY LAYER TRANSITION INDUCED BY A COHERENT PERTURBATION

H.C. DE LANGE AND R.J.M. BASTIAANS
Section Energy Technology, Department of Mechanical Engineering
Eindhoven University of Technology, The Netherlands

1. Abstract

Bypass transition of a boundary layer takes place at high main stream turbulence levels. It is governed by the intrusion of non-linear disturbances into the viscous sublayer. In this paper a numerical study is presented in which a spatially developing laminar boundary layer is subdued to large scale (non-linear) disturbances. The (fully compressible) Navier-Stokes equations are solved using direct numerical simulation with a higher order finite difference method on a collocated grid. The results show that the initially smooth disturbance rapidly changes into an arrow-head structure with the characterics of a turbulent spot.

2. Introduction

In the design of turbomachinery the prediction of the boundary layer layer heat transfer is of mayor importance, to since the hot gases from the combustion chamber force an enormous heat flux to the turbine blades. The heat transfer in a boundary layer increases significantly when laminar to turbulent transition occurs. When transition starts it is assumed that so called turbulent spots are initiated in the laminar boundary layer.

Turbulent spots have been first observed by (Emmons, 1951) in a water channel. Most transition models which are used nowadays are based on these turbulent spots. It is supposed that a turbulent spot is a local area of turbulence, that convects in streamwise direction with a mean velocity which is less than the main flow velocity. The leading edge travels faster than the trailing edge and so the turbulent spot grows lengthwise while moving in downstream direction. Furthermore, the spots appear to remain at the same shape so they also grow laterally. At a certain point the spots

start to merge untill the flow is completely turbulent. This is said to be the end of transition.

In general a distinction between natural and bypass transition must be made. At low disturbance levels in the main flow Tollmien-Schlichting waves are initiated at a certain Reynolds number. These waves grow in amplitude and three dimensional waves start to develop. Further downstream the first turbulent spots occur untill transition is completed. This scenario is called natural transition.

For higher turbulence levels bypass transition takes place. It is governed by the direct intrusion of non-linear disturbances into the viscous sublayer, where they initiate turbulent spots. In the spot-formation process both the length scale and the initial strength of the disturbance may be important.

Bypass transition is governed by the forcing of free-stream disturbances on the viscous sublayer. To describe bypass transition the transient growth theory has been developed over the last ten years. It can be modeled using the Parabolised Stability Equations. However, this modelling starts from the amplification of waves or (coherent) structures present in the boundary layer. There are two semi-emperical models ((Johnson, 1999) and (Mayle and Schultz, 1997)) known to describe the initiation for bypass transition starting from the intrusion of free-stream disturbances. In both models, the free-stream disturbances are assumed to intrude via the amplification and subsequent breakdown of laminar modes. The amplification rate is prescribed from emperical relations. The actual formation of turbulent spots (i.e. the onset of transition) has to be introduced through a presumed criterion.

These models result in the well-known intermittency distributions introduced in (Narashima, 1957) or (Johnson, 1994). In the derivation of these intermittency distributions the influence of the initation process only remains in the (empirical) parameter x_t (the streamwise position of the start of transtion). The shape of the distribution is determined by the spot growth- and merge-processes. This means that the theoretical models for natural and bypass transition both lead to these intermittency distributions, since they both lead to rapid non-linear breakdown and, therefore, more or less instantanious spotproduction. In the past numerous experiments have been performed to find Re_{xt} and Re_λ depending on the pressure gradient, turbulence intensity, compressibility, etc.

Recent experiments ((Schook *et al.*, 2001)) show that for low levels of free-stream turbulence the Narashima- and Johnson-intermittency distributions are indeed applicable. However, as the turbulence intensity is raised to levels representative for gasturbine flows, the intermittency distribution changes shape. A closer examination of the experimental conditions (at different levels and length scales of the free-stream turbulence) shows

that the Narashima- and Johnson-intermittency distributions are not found when the turbulence length scale is large compared to the boundary layer thickness.

The shape of the distributions, found at these length scales, suggests that 'spots' grow or shrink depending on both the local boundary layer thickness and the strength of the impinging disturbances. This means that the spots must be created directly from free-stream perturbations. They can not be the result of a initiation process within the boundary layer. Therefore, at these scales the mechanism of direct intrusion of free-stream disturbances dominates the initiation process.

This raises the question of boundary layer selectivity; which properties of a main stream disturbances are descisive for the production of a turbulent spot. In the present study fully compressible direct numerical simulation is used to study this transition mechanism. In this paper a numerical study is presented in which a spatially developing laminar boundary layer on a flat plate is subdued to large scale (non-linear) disturbances.

3. Governing equations

For a compressible flow of an ideal gas, conservation of mass, momentum and entropy can be written as

$$\begin{aligned} \frac{\partial \rho}{\partial t} + \nabla \cdot \rho \mathbf{v} &= 0 \\ \rho \left[\frac{\partial \mathbf{v}}{\partial t} + \mathbf{v} \cdot \nabla \mathbf{v} \right] &= -\nabla p - \nabla \cdot \boldsymbol{\tau} \\ \rho T \left[\frac{\partial s}{\partial t} + \mathbf{v} \cdot \nabla s \right] &= -\nabla \cdot \mathbf{q} - \boldsymbol{\tau} : \nabla \mathbf{v} \end{aligned} \tag{1}$$

with time t, density ρ, the velocity vector $\mathbf{v}$, entropy s, pressure p, stress tensor $\boldsymbol{\tau}$, temperature T and heatflux vector $\mathbf{q}$. The set of equations are closed with the constitutive relations $T = f(\rho, s)$ and $p = \rho RT$.
The use of the entropy s has the advantage that its conservation equation does not contain any acoustic waves. Therefore, only mass and momentum conservation need to be resolved on an acoustic time-scale.

4. Numerical scheme

The equations are solved with a higher order finite difference method on a collocated grid. The time integration uses a third order low storage Runge Kutta scheme, which requires only one additional storage location. A compact (implicit) sixth order scheme due to (?) is used for the spatial discretisation of all non-advective terms. The scheme uses five grid points and

can be evaluated with order N manipulations for N derivatives. Advection is approximated with a fifth order explicit upwind scheme. In this way a stable integration is obtained in which no additional filtering is required.

Characteristic boundary conditions are implemented according to the NSCBC approach of (?). In this approximation local one dimensional waves are used for acoustic and convective transport and supplemented with viscous conditions.

Sub-stepping is used in which acoustic, convective and viscous transport are evaluated in splitted (third and second-order) time evolution. The properties of the numerical scheme are such that it is ideal for parallel processing. Furthermore, the code is optimised for memory access, caching and load balancing. The calculations presented in this paper typically use about 400 CPU hours when run on 16 R10k3-processors (250 Mhz).

5. Problem definition

Initially a Blasius profile ($u_b(y)$, Ma_∞=0.1) is prescribed for Re_{δ^*} equal to 400 (with δ the momentum thickness, this means that the Reynolds-number based on the displacement thickness is approximately 1000). At the inflow boundary the wall normal velocity v is perturbed (similar as in (Breuer and Landahl, 1990), who used a spatially introduced streamwise vorticity) according to:

$$\begin{aligned}
\frac{\partial \mathrm{v}}{\partial t} &= Af(y)(1-2\phi^2)(1-2\xi^2)\exp(-\phi^2-\xi^2+1/2) \\
\phi &= \frac{t-t_0}{\theta} \qquad \theta = 11\delta^*/U_\infty \qquad t_0 = 6\theta \\
\xi &= \frac{z/L_z - 1/2}{\zeta} \qquad \zeta = 8 \\
f(y) &= u_b(y)(1-y/L_y)^2
\end{aligned}$$

The computation domain has a height L_y of $20\delta^*$, the length and width are choosen $6L_y$ and $3L_y$, respectively. The lateral length scale agrees with simulations by (Breuer and Landahl, 1990), who found that the resulting perturbation is approximately independent of the spanwise scale. The typical time-integration continues till tU_∞/δ^*=600. In the simulations a uniform grid of 193×65×192.

The flat plate is prescribed by an adiabatic no-slip boundary condition. The upper boundary is acoustically non-reflective. At the inflow the velocity components and entropy are fixed. At the outflow the downstream pressure is fixed. In the spanwise direction the domain is periodic.

6. Results

The initial perturbation results in a checkerboard pattern of (alternating) wall-normal velocity. This leads to three spanwise rows of three alternating negative/positive λ_2-pockets. In the main stream the disturbance is rapidly transferred to the outflow, as shown in figure 1, leaving behind a pattern of alternating positive and negative wall-normal velocity, with a characteristic length scale of δ^*. The formation of this pattern goes hand in hand with combination of the front middle and middle outer regions of negative λ_2 into an arrow-head structure, shown in figure 2. This structure is stretched into a lambda-shaped vortex, situated in the near-wall boundary layer region, below $3\delta^*$. The ratio of leading and trailing edge velocity of the lambda vortex is about 3. Subsequently, a rapid local creation of vortices near the legs is triggered, similar to the observations of (Singer and Joslin, 1994). In the later stages a turbulent spot-like structure is formed.

It is clear that the time-wise introduction of the perturbation on the wall-normal velocity leads to results very similar to those in (Breuer and Landahl, 1990). A difference in both results is the alternating pattern of wall-normal velocity at ther center-line which arises in the Breuer-results. It is not clear it these are caused by the difference in boundary conditions ((Breuer and Landahl, 1990) uses streamwise periodic boundary conditions). The similarity in the results indicates that the formulation of the initial disturbance ($v(t)$ instead of a spatial stream-wise vorticity perturbation) is not important. Instead the development of the initial disturbance into the Λ-vortex and the subsequent production of vorticity at the stretching legs seems to be determined by the perturbation-length scale. Of course, more simulations for different θ and ζ are needed to support this conclusion.

7. Conclusions

The results show that the developed code is suitable for the study of the spot-initiation proces. In the near future, the boundary layer sensitivity will be investigated for different θ and ζ. Furthermore, mode-selection for more random perturbations will be studied. These initial disturbance are placed in the laminar boundary layer. The intrusion mechanism of free-stream disturbances into the viscous sublayer will be the subject of future studies to answer the question of boundary layer selectivity.

References

Breuer, K.S. and Landahl, M.T. (1990) The evolution of a localized disturbance in a laminar boundary layer. Part 2. Strong disturbances *J. Fluid Mech.*, **Vol. no. 220**, pp. 595-621

Emmons, H.W. (1951) The laminar turbulent transition in a boundary layer *J. Aero. Sci.*, **Vol. no. 18**, pp. 490-498

Johnson, M.W. (1994) A bypass transition model for boundary layers *J. of Turbomachinery*, **Vol. no. 116**, pp. 759-764

Johnson, M.W. (1999) A physical model for bypass transition *J. Heat and Fluid flow*, **Vol. no. 20**, pp. 95-104

Lele, S.K., 1992 Compact finite difference schemes with spectral-like resolution *J. Comp. Phys.*, **Vol. no. 103**, pp. 16-42

Mayle, R.E., and Schultz, A. (1997) The path to predicting bypass transition *J. of Turbomachinery*, **Vol. no. 119(3)**pp. 405-411

Narashima, R. (1957) On the distribution of intermittency in the transition region of a boundary layer *J. Aero. Sci.*, **Vol. no. 24**, pp. 711-712

Poinsot, T.J. and Lele, S.K. (1992) Boundary conditions for direct simulations of compressible viscous flows *J. Comp. Phys.*, **Vol. no. 101**, pp. 104-129

Schook, R., Lange, H.C. de, and Steenhoven, A.A. van (2001) Heat transfer measurements in transitional boundary layers *Int. J. Heat and Mass Tr.*, **Vol. no. 44**, pp. 1019-1030

Singer, B.A., and Joslin, R.D. (1994) Metamorphosis of a hairpin vortex into a young turbulent spot *Physics of Fluids*, **Vol. no. 6**, pp. 3724-3736

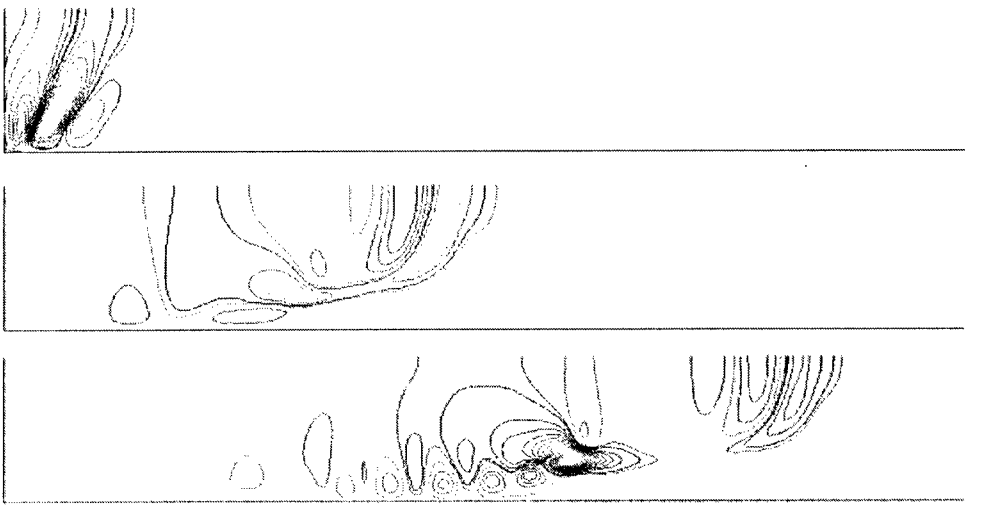

Figure 1. Contours of constant wall normal velocity on the center plane at $t = U_\infty/\delta^* = 98$, 245 and 392

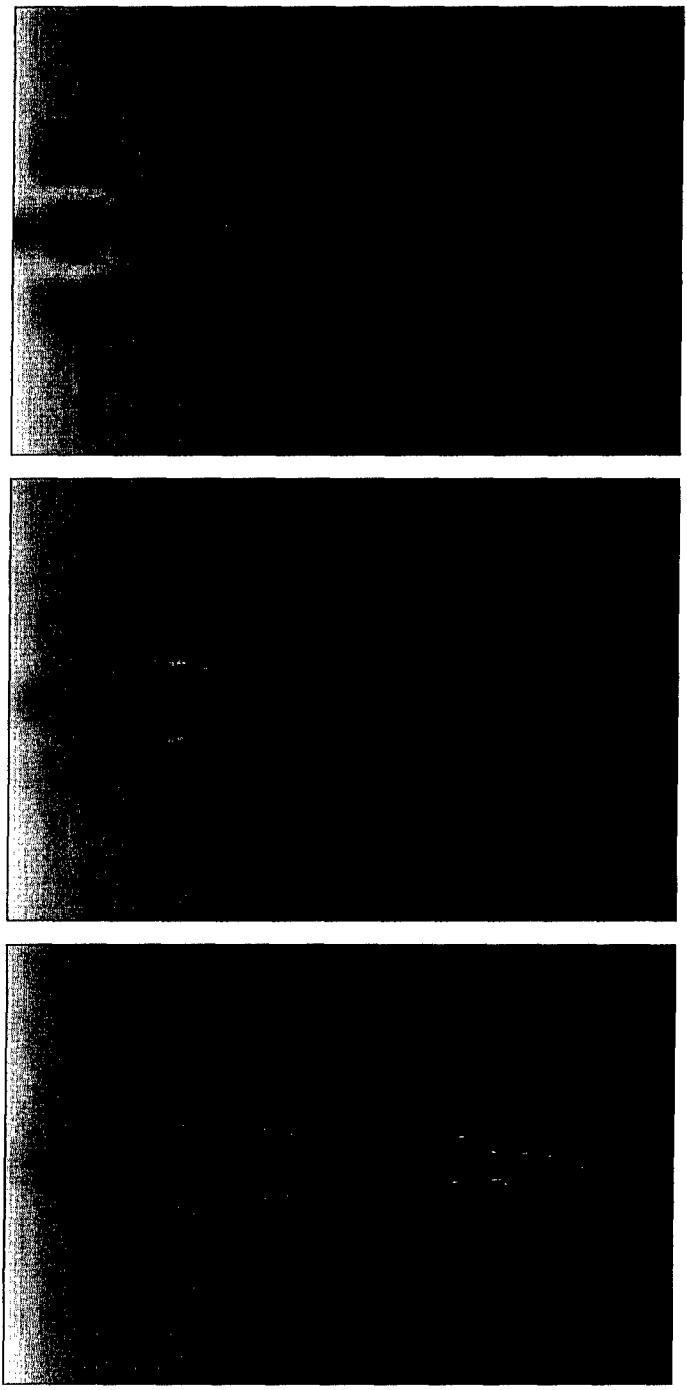

Figure 2. Top view of regions of negative λ_2 and gray scales indicating the entropy on the flat plate at tU_∞/δ^*=245, 392 and 539